chemosensors

Article

Noise Spectrum as a Source of Information in Gas Sensors Based on Liquid-Phase Exfoliated Graphene

Stevan Andrić, Ivana Jokić *, Jelena Stevanović, Marko Spasenović and Miloš Frantlović

Institute of Chemistry, Technology and Metallurgy—National Institute of the Republic of Serbia, University of Belgrade, 11000 Belgrade, Serbia; stevan@nanosys.ihtm.bg.ac.rs (S.A.); jelena@nanosys.ihtm.bg.ac.rs (J.S.); spasenovic@nanosys.ihtm.bg.ac.rs (M.S.); frant@nanosys.ihtm.bg.ac.rs (M.F.)

* Correspondence: ijokic@nanosys.ihtm.bg.ac.rs

Abstract: Surfaces of adsorption-based gas sensors are often heterogeneous, with adsorption sites that differ in their affinities for gas particle binding. Knowing adsorption/desorption energies, surface densities and the relative abundance of sites of different types is important, because these parameters impact sensor sensitivity and selectivity, and are relevant for revealing the response-generating mechanisms. We show that the analysis of the noise of adsorption-based sensors can be used to study gas adsorption on heterogeneous sensing surfaces, which is applicable to industrially important liquid-phase exfoliated (LPE) graphene. Our results for CO_2 adsorption on an LPE graphene surface, with different types of adsorption sites on graphene flake edges and basal planes, show that the noise spectrum data can be used to characterize such surfaces in terms of parameters that determine the sensing properties of the adsorbing material. Notably, the spectrum characteristic frequencies are an unambiguous indicator of the relative abundance of different types of adsorption sites on the sensing surface and their surface densities. We also demonstrate that spectrum features indicate the fraction of the binding sites that are already occupied by another gas species. The presented study can be applied to the design and production of graphene and other sensing surfaces with an optimal sensing performance.

Keywords: graphene-based gas sensor; sensor noise spectrum; sensing material characterization; heterogeneous sensing surface; adsorption–desorption process; carbon dioxide sensor

Citation: Andrić, S.; Jokić, I.; Stevanović, J.; Spasenović, M.; Frantlović, M. Noise Spectrum as a Source of Information in Gas Sensors Based on Liquid-Phase Exfoliated Graphene. *Chemosensors* **2022**, *10*, 224. https://doi.org/10.3390/chemosensors10060224

Academic Editor: Marina N. Rumyantseva

Received: 30 April 2022
Accepted: 11 June 2022
Published: 14 June 2022

1. Introduction

Gas sensing is a constantly expanding field in relation to the application of graphene and graphene-based materials [1–5]. Sensing structures made of such materials have a large specific surface area, and when exposed to the adsorption of gas particles, a pronounced change in their electrical and mechanical parameters can occur, resulting in a measurable sensor response even for extremely low adsorbed quantities [1,6]. Application of different chemical functionalizing elements, and the presence of structural defects in graphene, can significantly improve the sensing capabilities toward certain gas species [3,4,7,8]. The good gas sensing properties of liquid-phase exfoliated (LPE) graphene stem from its defect-rich structure, in the form of flakes with edges that have an abundance of highly reactive adsorption sites [9–11]. However, the existence of another type of adsorption site on the basal planes of the flakes makes the LPE graphene surface heterogeneous, requiring special attention in the analysis of measurement results. Knowing the values of the adsorption–desorption (AD) process parameters for different types of adsorption sites is essential in that sense. However, reliable data that can be applicable for gas sensing based on the use of LPE graphene, either theoretically or experimentally obtained, are still missing for many gases (including CO_2). In the existing literature, data can be found related to the adsorption energies for AD processes of various gases on pristine, functionalized, and

defective graphene, determined by the use of the density functional theory and other calculation methods [4]. However, their values for the same gas, and even for the same sensing surface are often different because they depend on the used calculation method, and on different effects and corrections that have been taken into account, and which more or less adequately correspond to a given situation and sensing surface [4,12]. Their applicability in the case of LPE graphene may be debatable given its specific structure, which consists of randomly arranged and irregularly shaped flakes with diverse edges.

Apart from LPE graphene, other gas sensing layers can be regarded as heterogeneous in the sense of having surface sites of different affinities for gas particles binding [13,14]. The causes of heterogeneity can be a non-uniform surface morphology, structure, or chemical composition, including the presence of various defects, irregularities, cavities, pores, impurities, different functional groups on the surface, or some other features that constitute surface inhomogeneity. An understanding of sensor heterogeneity is important for sensor characterization [15] but it can also be utilized for the optimization of sensor responses to different gas species [16]. Regardless of the nature of the heterogeneity, the adsorption properties of the sensing surface have to be characterized because they inherently influence the performance of the gas sensor. Apart from knowing the adsorption/desorption energies, it is also important to know the relative abundances of various adsorption site types on the surface, as they determine the dominant adsorption mechanism on which the sensor response rate and magnitude, sensitivity, selectivity, and sensing surface recovery depend. Such data therefore enable the optimization of the sensing performance during the design and fabrication of graphene-based surfaces and other sensing surfaces.

Apart from the usual gas detection methods, in which the temporal sensor response is measured and analyzed both in the transient regime and the steady state, new approaches have emerged which have improved the sensing performance. Spectrum analysis of the sensor noise, i.e., of the stochastic fluctuations of the sensor signal caused by the inherently random nature of the adsorption–desorption process of gas particles, has proven to be a promising (even superior) method for the detection and identification of gases in various types of adsorption-based sensors [17,18], including graphene gas sensors [19–21]. The main advantages of spectrum analysis are a higher sensitivity compared to conventional methods and an inherent selectivity and insensitivity to baseline drift [17,19,20].

In this work, as opposed to previous work on the use of the sensor noise spectrum for the detection and identification of gases, we present a new application of the analysis of the noise spectrum of a gas sensor with the sensing layer made of a heterogeneous material such as LPE graphene for characterizing the adsorption properties of the sensing surface. The main novelty of our work is a method to determine the relative abundance of different types of adsorption sites on the surface of an adsorbing material, the sites' surface densities, and the effective surface areas occupied by them and their numbers based on an analysis of measured noise. These data are lacking in the literature and are important for the development of adsorption sensors with an improved performance, and also for fundamental material research and the investigation of adsorption processes and mechanisms of interaction between different gases and surfaces. We used a mathematical model of noise developed for heterogeneous adsorption surfaces [22], and adapted its form to enable the extraction of the parameters that characterize the AD process on a surface with different types of adsorption sites. By using a CO_2 sensor as an example, we show that characteristic frequencies of the noise spectrum uniquely indicate the relative abundance of edge and basal plane adsorption sites on an LPE graphene surface, as well as the surface densities and numbers of the sites. CO_2 was chosen because there is a need to measure the concentration of that gas in a diverse field of applications. For example, CO_2 is an air pollutant and a greenhouse gas with a constantly increasing emission trend [23], which is causing global warming and the disruption of ecosystems. CO_2 is considered a non-toxic gas but it is harmful to health if an individual is exposed to it for a long time. There is a need in many industrial processes and in scientific research to measure CO_2 concentrations, with low concentrations also of interest [24]. In medicine, sensitive CO_2 sensors are desired

in capnography to detect disease at the early stages or to monitor the patient's physiological functions during anesthesia and some medical treatments [24]. Therefore, there is a need for a variety of CO_2 sensors, including highly sensitive sensors for trace amounts of CO_2, low cost and low energy consumption miniaturized gas sensors deployed in a dense network, sensors capable of real-time in situ measurements operating at room or ambient temperature, and those realized as flexible or wearable devices. Graphene gas sensors have great potential to meet the above requirements. Consequently, much research effort is being invested to use this material for CO_2 sensing, as evidenced by the volume of scientific literature dealing with this topic. Although very small detectable CO_2 concentrations have been reported using graphene sensors (e.g., [25–27]), in order to make the most of graphene as a sensing material, it is necessary to optimize the sensing layer with respect to both capturing gas molecules and the charge transfer between the gas particles and graphene (e.g., by using defect-rich graphene and surface functionalization). It is the investigation of the adsorbing properties of sensing materials that enables the characterization and optimization of the sensing performance during the design and fabrication of sensors for the detection of a particular gas. Thus, one of the objectives of the paper is to present a new way to characterize realistic heterogeneous adsorbing materials. CO_2 is taken as an exemplary gas, but the presented method is also applicable for other gases (including toxic gases such as SO_2 and NOx) and sensing surfaces (other types of graphene and graphene-based materials, other 2D materials, semiconductor oxides, etc.), and in cases when there is a greater number of adsorption site types.

2. Mathematical Model of Noise in Sensors with a Heterogeneous Sensing Surface

The heterogeneous active surface of adsorption-based gas sensors is defined by a spatial distribution of adsorption sites of different affinities towards a certain gas species. The general case assumes n ($n \geq 2$) types of adsorption sites on the surface, in which the adsorbing surface can be considered as consisting of a collection of locally homogeneous surface parts. The simplest heterogeneous surface has two distinct types of adsorption sites, and here it will be analyzed in detail. The case of a surface with three types of sites will also be considered. By assuming that only one gas particle can be bound to a single site of any kind, and that adsorbate particles do not interact among themselves, a multisite Langmuir model [28] for AD processes occurring on the surface can be applied, which has the form:

$$\frac{\mathrm{d}N_i}{\mathrm{dt}} = \frac{\alpha_i}{n_{mi}\sqrt{2\pi M k_B T}} p(N_{mi} - N_i) - \frac{1}{\overline{\tau}_i} N_i, \text{ for } i = 1 \text{ to } i = n. \tag{1}$$

Here the index "i" refers to the adsorption sites of the type I, N_i denotes the number of adsorbed gas particles, α_i is the sticking coefficient, N_{mi} is the number of the adsorption sites, n_{mi} is the sites surface density, p is the gas pressure, M is the mass of a single gas particle, T is the temperature, and k_B is the Boltzmann constant. The mean time a gas particle spends adsorbed on a site of the type i

$$\overline{\tau}_i = \tau_{0i} e^{\frac{E_{di}}{R_g T}} \tag{2}$$

depends on the desorption energy E_{di}, temperature, and the period of thermal vibrations of the adsorbed particle, τ_{0i} (R_g is the gas constant).

Equation (1) for each type of adsorption site yields the expressions for the time evolution of the number of adsorbed gas particles ($N_i(t)$), the number of adsorbed particles in the steady state of the AD process (N_{ie}), and the time constant with which the AD process approaches the steady state (τ_i):

$$N_i(t) = N_{ie}\left(1 - e^{-\frac{t}{\tau_i}}\right), \quad N_{ie} = \frac{b_i p}{1 + b_i p} N_{mi}, \quad \tau_i = \frac{\overline{\tau}_i}{1 + b_i p}, \tag{3}$$

where the parameter b_i equals

$$b_i = \frac{\alpha_i \overline{\tau}_i}{n_{mi}\sqrt{2\pi M k_B T}}. \quad (4)$$

The sensor time response can now be expressed as a sum of the components generated by the AD processes on different types of adsorption sites (r_i is the conversion factor of the number of adsorbed gas particles on the type i sites to the response):

$$R(t) = \sum_{i=1}^{n} r_i N_i(t) \quad (5)$$

$$R(t) = \sum_{i=1}^{n} r_i N_{ie}\left(1 - e^{-\frac{t}{\tau_i}}\right) \quad (6)$$

According to the previous expressions, the intrinsic sensor response (its kinetics, magnitude, rise time) in the presence of a certain gas in the sensor surroundings at a given temperature depends on the adsorption properties of the sensing surface for the given analyte. It is known that the response of adsorption-based sensors often does not strictly follow the single-exponential law due to different effects (e.g., the pronounced influence of mass transfer, the non-homogeneity of the sensing surface or parasitic adsorption due to non-ideal sensor selectivity) [29]. In experiments with graphene-based gas sensors, a rapid initial increase in the response has been observed, but the response approaches the steady state at a much slower rate, which is commonly attributed to different filling rates of high-affinity and low-affinity surface sites [30,31]. The kinetics of such a response is described by using two time constants, as predicted by Equation (6) for $n = 2$.

Due to the inherently stochastic nature of AD processes, the number of particles adsorbed on each type of adsorption site randomly fluctuates. These fluctuations, denoted by $\Delta N_i(t)$, result in fluctuations of the sensor's time response, $\Delta R(t)$:

$$\Delta R(t) = \sum_{i=1}^{n} r_i N(t) \quad (7)$$

which constitute the inevitable adsorption–desorption noise.

In order to obtain an analytical expression for the power spectral density (PSD) of the sensor AD noise, an analysis of the fluctuations in the numbers of adsorbed particles around steady-state values should be performed. The actual instantaneous number of adsorbed particles in the steady state fluctuates around N_{ie} as $N_i(t) = N_{ie} + \Delta N_i(t)$. Here we briefly present the derivation of the PSD of AD noise for the case of n types of sites on the sensing surface, based on the Langevin approach (as given in [22]). The n independent Langevin equations are obtained starting from the kinetic Equation (1):

$$\frac{\mathrm{d}\Delta N_i}{\mathrm{d}t} = -\frac{1}{\tau_i}\Delta N_i + \xi_i, \quad \text{for } i = 1 \text{ to } i = n \quad (8)$$

(ξ_i is a random source function). After solving Equation (8) in the frequency domain, we can obtain the PSD of fluctuations of the number of particles adsorbed on the type i sites:

$$S_{\Delta N_i}(f) = \frac{4N_{ie}\tau_i^2/\overline{\tau}_i}{1 + (f/f_{ci})^2}. \quad (9)$$

Since random processes $\Delta N_i(t)$ and $\Delta N_j(t)$ are statistically independent for every pair i and j, where $I \neq j$, the PSD of the sensor AD noise is obtained based on Equations (7) and (9) in the form of the sum of n lorentzians:

$$S_{\Delta R}(f) = \sum_{i=1}^{n} r_i^2 S_{\Delta N_i}(f) = \sum_{i=1}^{n} r_i^2 \frac{4N_{ie}\tau_i^2/\overline{\tau}_i}{1 + (f/f_{ci})^2}. \quad (10)$$

In particular, for the sensing surfaces with two types of adsorption sites, the previous expression, after some mathematical transformations, obtains the form:

$$S_{\Delta R}(f) = S_{LFNM}\frac{1+(f/f_{cC})^2}{[1+(f/f_{c1})^2][1+(f/f_{c2})^2]}, \tag{11}$$

that reveals three characteristic frequencies in the AD noise spectrum:

$$f_{ci} = \frac{1}{2\pi\tau_i} = \frac{1+b_i p}{2\pi\overline{\tau}_i}, \ \ i = 1 \text{ or } i = 2 \tag{12}$$

$$f_{cC} = \sqrt{\frac{r_1^2 N_{1e}\overline{\tau}_2 f_{c2}^2 + r_2^2 N_{2e}\overline{\tau}_1 f_{c1}^2}{r_1^2 N_{1e}\overline{\tau}_2 + r_2^2 N_{2e}\overline{\tau}_1}}, \tag{13}$$

and its low frequency noise magnitude:

$$S_{LFNM} = 4\left(r_1^2 N_{1e}\frac{\tau_1^2}{\overline{\tau}_1} + r_2^2 N_{2e}\frac{\tau_2^2}{\overline{\tau}_2}\right). \tag{14}$$

When there are three types of adsorption sites, the expression (10) for n = 3 can be transformed into:

$$S_{\Delta R}(f) = S_{LFNM,3}\frac{[1+(f/f_{cCI})^2][1+(f/f_{cCII})^2]}{[1+(f/f_{c1})^2][1+(f/f_{c2})^2][1+(f/f_{c3})^2]}, \tag{15}$$

where the frequencies f_{c1}, f_{c2}, and f_{c3} are given by the Equation (12) for i equal to 1, 2, or 3, the remaining two characteristic frequencies are determined by equations:

$$f_{cCI}^2 f_{cCII}^2 = \frac{(K_1+K_2+K_3)f_{c1}^2 f_{c2}^2 f_{c3}^2}{K_1 f_{c1}^2 + K_2 f_{c2}^2 + K_3 f_{c3}^2}, \tag{16}$$

$$f_{cCI}^2 + f_{cCII}^2 = \frac{(K_1+K_2)f_{c1}^2 f_{c2}^2 + (K_2+K_3)f_{c2}^2 f_{c3}^2 + (K_1+K_3)f_{c1}^2 f_{c3}^2}{K_1 f_{c1}^2 + K_2 f_{c2}^2 + K_3 f_{c3}^2}, \tag{17}$$

$$K_i = 4r_i^2 N_{ie}\frac{\tau_i^2}{\overline{\tau}_i}, \ \ i = 1,2,3, \tag{18}$$

and the low frequency noise magnitude is:

$$S_{LFNM,3} = K_1 + K_2 + K_3. \tag{19}$$

Here we notice that Equations (13) and (14) can be expressed in the form:

$$f_{cC}^2 = \frac{(K_1+K_2)f_{c1}^2 f_{c2}^2}{K_1 f_{c1}^2 + K_2 f_{c2}^2}, \tag{20}$$

$$S_{LFNM} = K_1 + K_2, \tag{21}$$

where all the quantities are already defined.

The mathematical models given by the presented expressions will be used in our further analysis.

3. Results and Discussion

We investigated the applicability of noise spectrum analysis for the characterization of heterogeneous sensing surfaces by considering a carbon dioxide-resistive sensor based on LPE graphene, assuming that there are two types of adsorption sites: those on the edges of graphene flakes (type 1 sites), and those on their basal planes (type 2 sites) [10]. Type 1

sites account for a relatively small proportion of the total sensing area, while type 2 sites are located on its major part. Adsorption on both types of sites contributes to the sensor response and its fluctuations, while the response time and magnitude, as well as the noise spectrum characteristic features, depend on the reactivity of each type of site for the target gas and the surface densities of the sites and their relative abundance on the sensing surface. We performed the theoretical simulation based on the presented theoretical model, by using the values of the parameters obtained with DFT calculations found in the literature. The results will be compared in specific aspects with experimental and simulation data from the literature.

It is known that the adsorption of carbon dioxide and other gas molecules on a pristine graphene surface is based on a weak physical interaction, yielding a very low sensor signal [4,32]. It can be assumed that the same is also valid for adsorption sites located on non-defective basal planes of graphene flakes. The reactivity of edge sites is much higher, so the adsorption on such sites constitutes the main contribution to the sensor response. If a large part of the graphene surface, corresponding to basal planes, could be utilized more effectively, the response magnitude and the sensor sensitivity would be significantly improved. Experiments and numerous theoretical studies have shown that a significant improvement in graphene reactivity toward various gases can be achieved by using different strategies, including the doping or decoration of graphene, where various atoms, molecules, functional groups, or nanoparticles were used [4,23,33,34]. Therefore, we will assume that the graphene is chemically functionalized in order to maximize the use of its adsorption surface. Together with the presence of a multitude of edge adsorption sites, this significantly improves the response to carbon dioxide. Adsorption of CO_2 on graphene functionalized with different elements has been investigated by using the DFT method, and the results show that a very strong interaction (i.e., strong chemical adsorption) has been achieved in some cases [33,35–39]. However, it is necessary to take into account that in the case of strong adsorption, the reusability of the sensor becomes an issue because the regeneration of the sensing surface for subsequent measurements requires the efficient and complete desorption of gas particles. Thus, the best choice for functionalization are elements that exhibit a sufficiently strong but, at the same time, reversible interaction between the sensing surface and the target molecules. Based on the previous considerations, it is reasonable for the AD noise analysis to assume the energy E_{d2} = 12.5 kcal/mol for CO_2 binding to functionalized basal plane sites, which is obtained by the density functional theory calculations in [40]. That study describes the adsorption of CO_2 molecules on a Fe-functionalized graphene sheet. It also reports the charge transfer of 0.02 electrons per adsorbed CO_2 molecule. LPE graphene flakes generally have edge structures that are a combination of different geometries. CO_2 adsorption on edge defects was analyzed on graphene nanoribbons, considering different edge types: basic zigzag and armchair, and their variations [32,41–43]. Some DFT calculations resulted in very high binding energy values (typically on zigzag edges, e.g., 89.5 kcal/mol [32]), indicating strong chemical adsorption, which is irreversible. It is clear that irreversible adsorption on such highly reactive adsorption sites does not contribute to fluctuations of gas particles after the steady state has been established, which makes such sites irrelevant for AD noise analysis. Moderately strong CO_2 binding has been reported for the zigzag (57) and armchair adsorption sites of graphene nanoribbons, with the binding energy of approximately 19 kcal/mol [43]. The forming of these kinds of edges has proven to be energetically favorable in graphene nanoribbons [44,45]. In the analysis of the contribution of LPE graphene edge adsorption to the sensor AD noise, we will therefore use the value E_{d1} = 19 kcal/mol.

The principle of operation of resistive sensors is based on an adsorption-induced change in the graphene electrical conductivity through the charge transfer interactions between the graphene and the adsorbate. Thus, in such sensors, gas adsorption experiments are performed by measurements of the electrical conductance of the sensing layer, and in sensor noise analysis, the power spectral density of the conductance fluctuations is a

quantity of interest. The effective change in the conductivity of the sensing layer, σ, is proportional to the total change in the number of free charge carriers in the adsorbing material, N_{CH}, which is determined by the number of adsorbed gas molecules at each type of site, N_i, and the corresponding charge transfer per adsorbed molecule, w_i [46]. For two types of sites, the proportionality $\sigma \sim N_{CH}$ becomes $\sigma \sim (N_1 w_1 + N_2 w_2)$. A change in the conductivity of the sensing layer $G \sim \sigma$ can be represented by the expression $G = kN_{CH} = k(N_1 w_1 + N_2 w_2)$, where the constant k depends on the electron charge, the charge carrier mobility, and the geometric parameters of the sensing layer (as introduced in [14], except that here $w_1 \neq w_2$). Considering that the time response of the sensor is a change in the conductivity of the sensing layer over time, in accordance with the notation introduced in Section 2, the sensor response defined by expression (5) is now $R(t) = G$, which implies $r_1 = kw_1$ and $r_2 = kw_2$. Therefore, the PSD of the sensor noise (Equation (10)) is the PSD of the conductance fluctuations:

$$S_{\Delta R}(f) = S_{\Delta G}(f) = \sum_{i=1}^{2} r_i^2 S_{\Delta N_i}(f) = \sum_{i=1}^{2} r_i^2 \frac{4N_{ie}\tau_i^2/\overline{\tau}_i}{1 + (f/f_{ci})^2}. \quad (22)$$

The conductance fluctuations spectrum can also be expressed as:

$$S_{\Delta R}(f) = S_{\Delta G}(f) = k^2 \sum_{i=1}^{2} w_i^2 S_{\Delta N_i}(f) = k^2 S_{\Delta N_{CH}}(f), \quad (23)$$

where $S_{\Delta NCH}(f)$ is the PSD of fluctuations of the number of charge carriers included in the charge transfer between the adsorbed molecules and the sensing material:

$$S_{\Delta N_{CH}}(f) = \sum_{i=1}^{2} w_i^2 S_{\Delta N_i}(f) = \sum_{i=1}^{2} w_i^2 \frac{4N_{ie}\tau_i^2/\overline{\tau}_i}{1 + (f/f_{ci})^2}. \quad (24)$$

This last quantity is the most suitable to illustrate the method of characterization of the heterogeneous sensing layer, which we present in this paper, where we make use of the characteristic frequencies of the noise spectrum. Namely, the PSD of sensor noise, i.e., the PSD of the fluctuations of the conductance of the sensing layer (which would be determined experimentally), $S_{\Delta G}(f)$, is proportional to $S_{\Delta NCH}(f)$, so the corresponding characteristic frequencies of these PSDs are the same. The difference between these two spectra is only in the noise magnitude (they differ by the constant factor k^2), which is not important for the method we present, because it uses values of characteristic frequencies of the noise spectrum. The spectrum $S_{\Delta NCH}(f)$ that we have analyzed for the given gas pressure and temperature depends only on the adsorption properties of the sensing material for a given gas and does not require knowledge of the geometric parameters of the sensing layer, which do not affect the characteristic frequencies of the noise spectrum, as can be seen from Equations (12) and (13). It is obvious that in Equation (12) there is no dependence on the constant k. That k does not exist in Equation (13) becomes clear after replacing $r_1 = kw_1$ and $r_2 = kw_2$, because k in the numerator and denominator of expression (13) is canceled. If the sensor output signal were current or voltage, the sensor noise would be current or voltage fluctuations, and their PSD would also be proportional to $S_{\Delta NCH}(f)$, so an analysis of $S_{\Delta NCH}(f)$ is optimal to demonstrate the method. Proportionality of noise, i.e., the fluctuations of the sensing layer electrical conductivity or resistance, as well as the sensor output current or voltage to the PSD of the fluctuations of the number of particles is also presented and used in [17,18,46]. For these reasons, in this paper we analyze the PSD of the number of carriers included in the charge transfer.

Characterization of the adsorbing surface with the method we present here (as well as other methods based on measurement and analysis of noise spectrum) is performed in the atmosphere of a single gas (in this case CO_2), at a constant gas concentration and constant temperature in a steady state. Sensor signal fluctuations (i.e., noise) are usually analyzed in the frequency domain, in which noise is represented by its power spectral density, which

in the literature is usually simply referred to as the noise spectrum. Figure 1a shows the AD noise power spectrum for various ratios of the numbers of adsorption sites of two types, $v = N_{m1}/N_{m2}$, N_{m1} being the number of adsorption sites on the edges, and N_{m2} the number of basal plane sites (the gas concentration is 1 ppm, T = 300 K, and the total sensing surface area is 10 × 10 mm^2, i.e., $A = 10^{-4}$ m^2). It is given as the power spectral density of fluctuations in the number of electrons included in the charge transfer between the adsorbed CO_2 molecules and the sensing material. The characteristic features of the spectrum (two knees, one inflection point, and the low-frequency noise magnitude) are visible for all values of v for the given parameter set. The characteristic features become more distinguishable after the multiplication of the spectrum with the Fourier frequency f, as shown in Figure 1b. The resulting quantity ($f \cdot S_{\Delta R}(f)$) is commonly used for the analysis of experimentally obtained noise spectra of graphene gas sensors [19,20]. Measurements in the shown frequency range can routinely be performed with a spectrum analyzer.

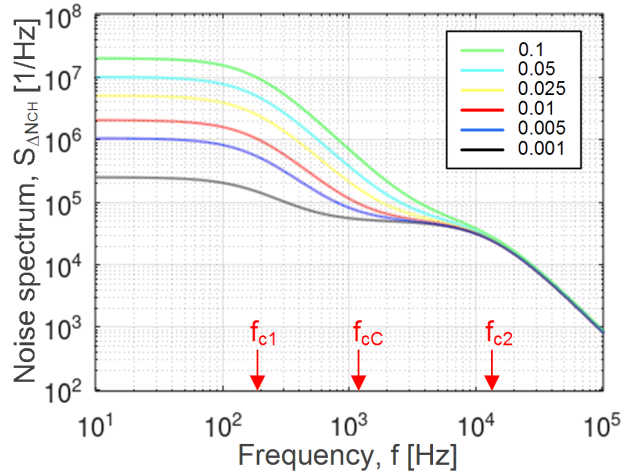

(**a**)

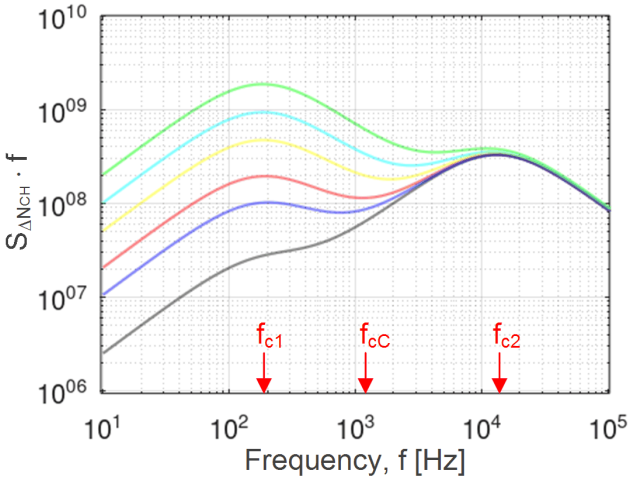

(**b**)

Figure 1. (**a**) Noise spectrum, i.e., the power spectral density of fluctuations in the number of electrons included in the charge transfer between the adsorbed CO_2 molecules and the heterogeneous sensing material, for various ratios v of the number of adsorption sites on the edges and the number of basal plane sites of LPE graphene. (**b**) The same quantity multiplied by the frequency f, thus making the spectrum characteristic features more distinguishable. The characteristic frequencies of the spectrum are shown for the case v = 0.01 (red curve).

Figure 2a shows the dependence of the noise spectrum characteristic frequencies on the ratio of the total number of adsorption sites on the edges and the total number of

sites on basal planes of LPE graphene flakes. It can be seen that the value of the central characteristic frequency f_{cC} unambiguously indicates the relative abundance v of different types of adsorption sites, while the frequencies f_{c1} and f_{c2} are unaffected by v.

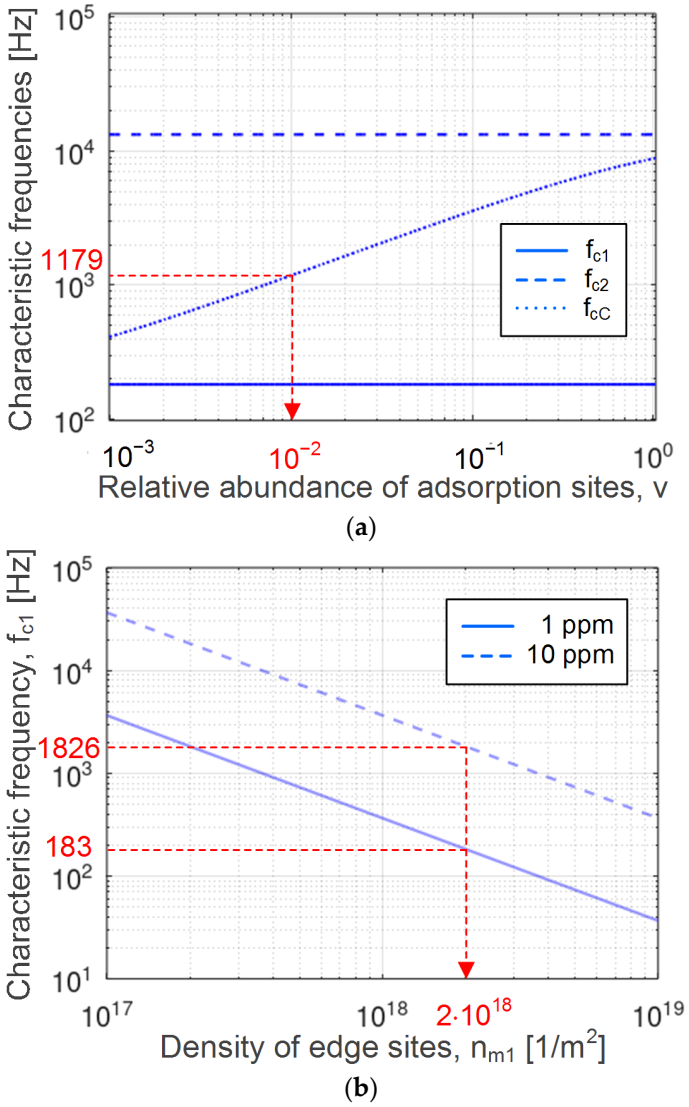

Figure 2. (**a**) Dependence of the noise spectrum characteristic frequencies on the ratio of the numbers of edge and basal plane sites, v (the other parameter values are the same as for Figure 1). It is shown that the value f_{cC} = 1179 Hz unambiguously indicates that v = 0.01 (in accordance with the red curves in Figure 1), (**b**) Characteristic frequency corresponding to the spectrum noise component that originates from the fluctuations of the number of gas particles on edge adsorption sites, as a function of the density of the sites, for two different CO_2 concentrations. The values of f_{c1} for different concentrations uniquely determine the density of edge sites on the same sensing surface, as shown in red.

The characteristic frequency f_{c1}, corresponding to the noise spectrum component that originates from the fluctuations in the number of gas particles on edge adsorption sites, as a function of the site's density n_{m1}, is shown in Figure 2b for two different CO_2 concentrations (1 ppm and 10 ppm). The values of f_{c1} for different concentrations uniquely determine the density of the edge sites on the same sensing surface, as shown in the diagram (values in red color). The dependence shown in Figure 2b is dictated by Equation (12). It shows that the frequency f_{c1}, at any given concentration (i.e., pressure) of gas, unambiguously indicates the density of the adsorption sites. Thus, at other concentrations as well (e.g.,

1000 ppm or 1 ppb), the corresponding values of the frequency f_{c1} will result in the same value of n_{m1}, which is the property of the adsorbing surface.

The results presented in Figs. 1a and 1b and the theory given in Section 2 show that it is possible to determine the characteristic frequencies f_{c1}, f_{c2}, and f_{cC} from the experimentally obtained noise spectrum at known pressure and temperature values. The noise measurements were performed in stable conditions, after the establishment of the steady state. The time of establishing of the steady state is determined by the largest time constant of the AD processes at different adsorption sites (in our analysis approximately 4 ms). By using the diagram $f_{c1}(n_{m1})$, which was obtained theoretically based on Equation (12) for a given gas pressure, temperature, and energy E_{d1}, n_{m1} was determined that corresponded to the experimentally obtained value f_{c1}. For an illustration of the procedure, first the value f_{c1} = 183 Hz, denoted in Figure 2b, was obtained from Figure 1b (red curve), and then the matching value $n_{m1} = 2{\cdot}10^{18}$ m^{-2} was read out from Figure 2b. Similarly, from the theoretical dependence $f_{c2}(n_{m2})$ defined by Equation (12), n_{m2} was obtained based on the experimentally determined value f_{c2}. The diagram $f_{cC}(v)$ was obtained theoretically, based on Equation (13) for the previously obtained parameter values f_{c1}, f_{c2}, n_{m1}, and n_{m2} (with the introduced substitution $N_{m1} = vN_{m2}$). The dependence $f_{cC}(v)$ enabled the determination of the relative abundance v of the two types of adsorption sites for an experimentally obtained value f_{cC}. As illustrated in Figure 2a, for f_{cC} = 1179 Hz, obtained from the red curve shown in Figure 1b, v equaled 0.01. The total number of the basal plane adsorption sites was obtained as $N_{m2} = n_{m2}A_2$, where $A_2 = An_{m1}/(n_{m1} + vn_{m2})$ is the surface area of the basal planes (the expression is derived from $A = A_1 + A_2 = N_{m1}/n_{m1} + N_{m2}/n_{m2}$). Thus, $N_{m2} = 3.992{\cdot}10^{13}$, and the average surface density of the basal plane sites on the entire sensing surface was $n_{m2t} = N_{m2}/A = 3.992{\cdot}10^{17}$ m^{-2}. Now, by using the already determined N_{m2} and v values, the total number of edge sites was calculated as $N_{m1} = vN_{m2}$, yielding the value $3.992{\cdot}10^{11}$, and the average surface density of the edge sites on the entire sensing surface was $n_{m1t} = N_{m1}/A = 3.992{\cdot}10^{15}$ m^{-2}. The ratio N_{m1}/n_{m1} is a measure of the effective surface area occupied by the edge binding sites. For the parameter values used in the presented analysis, this surface area was 0.2% of the total sensing surface area. For comparison, by fitting the bi-Langmuir adsorption model to the experimental results for the adsorption of acetone on graphene, the high-energy sites accounted for 0.24% of the total surface area of graphene, and DFT calculations revealed that such sites are localized on the surface steps formed by the edges of graphene flakes lying on the basal planes of the layer below them [47].

In [40], the adsorption of CO_2 on Fe-functionalized graphene in an oxygen environment was studied in detail in order to determine the influence of the strong (irreversible) adsorption of O_2 molecules on the sensing properties of the adsorbing material regarding CO_2. The co-adsorption of the two molecular species was analyzed, i.e., binding of CO_2 and O_2 molecules to the same adsorption site. By using DFT calculations, it was found that the binding energy of a CO_2 molecule after O_2 capture was 8.07 kcal/mol (compared to 12.5 kcal/mol when CO_2 is adsorbed directly to the functionalized surface site), and that it resulted in a net charge transfer of approximately 0.1 e per adsorbed molecule. Thus, the sensor response to CO_2 remained, although CO_2 molecules prefer oxygen-free adsorption sites. In order to correctly interpret the measurement results obtained in the case of carbon dioxide detection in an oxygen environment, the fraction of surface sites occupied by O_2 molecules must be known. For this reason, we expanded the noise model to take into account the adsorption of CO_2 molecules on adsorption sites occupied by O_2 molecules, which can be considered as the third type of adsorption sites. By using the parameter values obtained by DFT in [40], the diagram shown in Figure 3 was obtained.

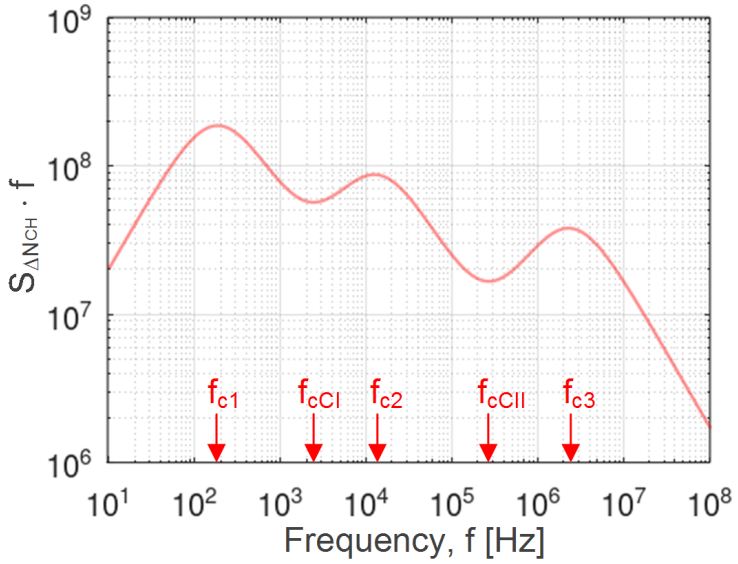

Figure 3. Noise spectrum (the power spectral density of fluctuations of the number of electrons included in the charge transfer between the adsorbed CO_2 molecules and the heterogeneous sensing material) multiplied by the frequency. There are three types of adsorption sites since, apart from edge and oxygen-free basal plane sites, functionalized sites occupied by O_2 molecules are considered. Five characteristic spectrum features (three maxima and two minima) are clearly distinguishable. The five characteristic frequencies of the spectrum are shown.

In the diagram (Figure 3) showing the noise spectrum multiplied by the frequency, five characteristic features (three maxima and two minima) can be identified, which can be used as a source of information about the abundance of different types of adsorption sites. Namely, the experimentally obtained spectrum enabled the determination of five characteristic frequencies, in accordance with the theoretical model (Equation (15)). Then the obtained values f_{c1} = 183 Hz, f_{c2} = 13.22 kHz, and f_{c3} = 2.347 MHz directly enabled the determination of the surface density of edge sites, and of basal plane adsorption sites without and with bound O_2 molecules, $n_{m1} = 2{\cdot}10^{18}$ m^{-2}, $n_{m2} = 4{\cdot}10^{17}$ m^{-2} and $n_{m3} = 4{\cdot}10^{17}$ m^{-2}, respectively. For this purpose, the theoretical dependences $f_{c1}(n_{m1})$, $f_{c2}(n_{m2})$ and $f_{c3}(n_{m3})$ were used for given gas pressure, temperature, and energies E_{d1}, E_{d2}, and E_{d3}, as explained before (Equation (12)). The two remaining characteristic frequencies, for which the obtained values were f_{cCI} = 2.31 kHz and f_{cCII} = 264.27 kHz, revealed the ratio of the numbers of the edge sites and basal plane sites free of oxygen molecules, v_{12} = 0.04, and also the ratio of the numbers of basal plane sites occupied and unoccupied by O_2 molecules, v_{32} = 3, by using Equations (16)–(18), where we introduced $v_{12} = N_{m1}/N_{m2}$ and $v_{32} = N_{m3}/N_{m2}$ after the division of both the numerator and the denominator of Equations (16) and (17) by N_{m2}. Since the surface area covered by oxygen-free basal plane sites was $A_2 = An_{m1}n_{m3}/(n_{m1}n_{m3} + v_{12}n_{m2}n_{m3} + v_{32}n_{m1}n_{m2})$ (the expression was derived from $A = A_1 + A_2 + A_3 = N_{m1}/n_{m1} + N_{m2}/n_{m2} + N_{m3}/n_{m3}$), the number of such sites was $N_{m2} = n_{m2}A_2 = 9.98{\cdot}10^{12}$, while the number of basal plane adsorption sites occupied by oxygen molecules was $N_{m3} = v_{32}N_{m2} = 2.994{\cdot}10^{13}$. The obtained values show that 75% of basal plane adsorption sites were occupied by O_2 molecules. The total number of basal plane sites was $N_{mb} = N_{m2} + N_{m3} = 3.992{\cdot}10^{13}$, so the ratio of the number of edge sites to the number of basal plane sites is $v = N_{m1}/N_{mb} = 0.01$.

Our results show that noise data can be used for the characterization of a heterogeneous adsorption surface of LPE graphene in terms of the parameters that determine the sensing properties of the material. Namely, material properties affect noise only in the sense that there are several different adsorption sites on a heterogeneous sensor surface, where AD processes occur, randomly by nature, as a result of which the number of adsorbed particles on each type of site fluctuates randomly, producing fluctuations in sensing layer

conductivity, i.e., sensor output signal fluctuations (sensor noise). The parameters of the AD process are characteristic to a given material and gas (adsorption/desorption energy, density, and number of adsorption sites of different types) and can be determined by noise spectrum analysis. The characterization of the adsorption surface using the proposed method was performed in the atmosphere of a single gas at a single given concentration, in the steady state. The method is based on a theoretical model that takes into account the adsorption of a single gas on a heterogeneous surface. If applied separately to two gases, the adsorption properties of the surface can be characterized for each gas individually. The characterization of the simultaneous adsorption of multiple gases from a mixture, which would allow the selectivity of the sensor to be assessed, requires an extension of the presented theoretical model, which will be the subject of future research. Apart from the determination of the above-mentioned parameters from the characteristic frequencies, the analysis that includes the low frequency noise magnitude combined with the sensor temporal response also enables the experimental determination of other parameters, e.g., the binding energies for CO_2 adsorption on LPE graphene, which are also lacking in the literature. Measurements at several different temperatures can also provide a greater diversity and number of parameters that can be obtained from the noise spectrum. For example, it would be possible to determine how much the adsorption of a single gas particle on each site type contributes to the sensor response. In cases where more than three types of adsorption sites exist, the mathematical transformation of the obtained analytical expressions for noise PSD can be used for the modeling of additional characteristic features that are visible in the noise spectrum, thus yielding more information about adsorption on a given sensing surface. Such approaches will be investigated in our future research.

4. Conclusions

We presented the model of sensor noise, i.e., of stochastic fluctuations of the sensor output signal, which are caused by inherently random adsorption–desorption processes on a heterogeneous sensing surface. It is applicable to surfaces with an arbitrary number of types of adsorption sites that differ in both the affinity toward the target gas and the contribution to the sensor signal. The importance of the model stems from the fact that for many sensors based on nanomaterials or thin films, this is a more realistic scenario than an ideally homogeneous surface. A heterogeneous surface must be characterized before it can be used for sensing, because its adsorption properties inherently affect gas sensor performance. For the cases of two and three types of adsorption sites, we obtained the models in the form that enabled an identification of all characteristic features of an experimentally obtained noise spectrum, which are useful for the characterization of adsorption properties of a complex surface. Our model allows the relative abundance of the different adsorption site types to be tuned, which makes it applicable to surfaces that are nearly perfectly homogeneous, as well as those that are highly heterogeneous. The model was applied in the analysis of the noise spectra of graphene gas sensors produced by liquid-phase exfoliation (LPE), knowing that the material has different types of adsorption sites on the edges and basal planes of graphene flakes. In our analysis, we used parameter values from the literature, which were obtained based on the density functional theory (DFT) calculations for the adsorption of carbon dioxide on graphene.

We have shown for the first time that the noise spectrum is a valuable source of information for the characterization of heterogeneous sensing surfaces. In particular, the noise spectrum can be used to quantify sensor surface parameters such as the relative abundance of adsorption sites of different types, and the surface density and number of edge and basal plane sites. We also applied our model in order to determine the extent of the occupation of adsorption sites by highly reactive species from the environment, which changes the adsorption properties of the sensing surface by reducing the initial number of adsorption sites, and introduces a new site type on which target gas molecules can be co-adsorbed together with the reactive species. While the mentioned parameters are obtained only from the spectrum characteristic frequencies, the analysis that includes the

low frequency noise magnitude and the sensor temporal response enables the experimental determination of other parameters that influence sensing performance. That includes, for example, the binding energies for CO_2 adsorption on LPE graphene, which are also lacking in the literature.

Although in this work we studied the adsorption of CO_2 gas on the surface of LPE graphene, our model and the analysis procedure can be applied to sensors made of other materials and/or for other gases. Such a surface characterization method is useful for understanding and designing, for example, nanomaterial-based sensors, or semiconductor sensors with various types of intentionally introduced or spontaneously occurring surface inhomogeneity. The presented noise model is also applicable for the limiting performance estimation of sensors with a heterogeneous surface. We expect our findings to be proven as valuable for the design of novel gas sensors and detection methods based on noise spectrum analysis.

Author Contributions: Conceptualization, I.J., M.F. and M.S.; investigation, S.A. and I.J.; methodology, M.F., I.J. and M.S.; software, S.A. and I.J.; formal analysis, S.A., M.S. and M.F.; writing—original draft preparation, S.A., I.J., M.S. and M.F.; visualization, S.A., I.J. and J.S.; project administration, M.S. and M.F.; funding acquisition, M.S.; validation, I.J. and J.S.; supervision, M.F. All authors have read and agreed to the published version of the manuscript.

Funding: This research was funded by the Science Fund of the Republic of Serbia, grant number 6057070, project Gramulsen, and by the Ministry of Education, Science, and Technological Development of the Republic of Serbia, project TR32008 and grant number 451-03-68/2022-14/200026.

Conflicts of Interest: The authors declare no conflict of interest.

References

1. Zhang, J.; Liu, L.; Yang, Y.; Huang, Q.; Li, D.; Zeng, D. A review on two-dimensional materials for chemiresistive- and FET-type gas sensors. *Phys. Chem. Chem. Phys.* **2021**, *23*, 15420–15439. [CrossRef] [PubMed]
2. Wang, T.; Huang, D.; Yang, Z.; Xu, S.; He, G.; Li, X.; Hu, N.; Yin, G.; He, D.; Zhang, L. A Review on Graphene-Based Gas/Vapor Sensors with Unique Properties and Potential Applications. *Nano-Micro Lett.* **2016**, *8*, 95–119. [CrossRef] [PubMed]
3. Tang, X.; Debliquy, M.; Lahem, D.; Yan, Y.; Raskin, J.-P. A Review on Functionalized Graphene Sensors for Detection of Ammonia. *Sensors* **2021**, *21*, 1443. [CrossRef] [PubMed]
4. Cruz-Martínez, H.; Rojas-Chávez, H.; Montejo-Alvaro, F.; Peña-Castañeda, Y.A.; Matadamas-Ortiz, P.T.; Medina, D.I. Recent Developments in Graphene-Based Toxic Gas Sensors: A Theoretical Overview. *Sensors* **2021**, *21*, 1992. [CrossRef] [PubMed]
5. Varghese, S.S.; Lonkar, S.; Singh, K.K.; Swaminathan, S.; Abdala, A. Recent advances in graphene based gas sensors. *Sens. Actuators B* **2015**, *218*, 160–183. [CrossRef]
6. Schedin, F.; Geim, A.K.; Morozov, S.V.; Hill, E.W.; Blake, P.; Katsnelson, M.I.; Novoselov, K.S. Detection of individual gas molecules adsorbed on graphene. *Nat. Mater.* **2007**, *6*, 652–655. [CrossRef]
7. Nemade, K.R.; Waghuley, S.A. Role of Defects Concentration on Optical and Carbon Dioxide Gas Sensing Properties of Sb2O3/Graphene Composites. *Opt. Mater.* **2014**, *36*, 712–716. [CrossRef]
8. Andrić, S.; Sarajlić, M.; Frantlović, M.; Jokić, I.; Vasiljević-Radović, D.; Spasenović, M. Carbon Dioxide Sensing with Langmuir–Blodgett Graphene Films. *Chemosensors* **2021**, *9*, 342. [CrossRef]
9. Ricciardella, F. From Graphene to Graphene-Based Gas Sensors Operating in Environmental Conditions. Ph.D. Thesis, Università degli Studi di Napoli Federico II, Naples, Italy, 2015. Available online: http://www.fedoa.unina.it/10129/1/Ricciardella_Filiberto_27.pdf (accessed on 30 April 2022).
10. Ricciardella, F.; Massera, E.; Polichetti, T.; Miglietta, M.L.; Di Francia, G. A calibrated graphene-based chemi-sensor for sub parts-per-million NO_2 detection operating at room temperature. *Appl. Phys. Lett.* **2014**, *104*, 183502. [CrossRef]
11. Tomašević-Ilić, T.; Jovanović, Đ.; Popov, I.; Fandan, R.; Pedrós, J.; Spasenović, M.; Gajić, R. Reducing sheet resistance of self-assembled transparent graphene films by defect patching and doping with UV/ozone treatment. *Appl. Surf. Sci.* **2018**, *458*, 446–453. [CrossRef]
12. Montejo-Alvaro, F.; Oliva, J.; Herrera-Trejo, M.; Hdz-García, H.; Mtz-Enríquez, A.I. DFT study of small gas molecules adsorbed on undoped and N-, Si-, B-, and Al-doped graphene quantum dots. *Theor. Chem. Acc.* **2019**, *138*, 37. [CrossRef]
13. Tamilarasan, P.; Ramaprabhu, S. Effect of partial exfoliation in carbon dioxide adsorption-desorption properties of carbon nanotubes. *J. Appl. Phys.* **2014**, *116*, 124314. [CrossRef]
14. Liang, S.-Z.; Chen, G.; Harutyunyan, A.R.; Cole, M.W.; Sofo, J.O. Analysis and optimization of carbon nanotubes and graphene sensors based on adsorption-desorption kinetics. *Appl. Phys. Lett.* **2013**, *103*, 233108. [CrossRef]
15. Gautam, S.K.; Panda, S. Effect of Surface Heterogeneity, Heat of Adsorption and Surface Area on the Characteristics of PANI-SnO_2 Based H_2S Gas Sensor. In Proceedings of the AIChE Annual Meeting, Virtual, 16–20 November 2020. Avail-

able online: https://www.aiche.org/academy/conferences/aiche-annual-meeting/2020/proceeding/paper/152g-effect-surface-heterogeneity-heat-adsorption-and-surface-area-on-characteristics-pani-sno2 (accessed on 30 April 2022).
16. Yang, D.; Fuadi, M.K.; Kang, K.; Kim, D.; Li, Z.; Park, I. Multiplexed Gas Sensor Based on Heterogeneous Metal Oxide Nanomaterial Array Enabled by Localized Liquid-Phase Reaction. *ACS Appl. Mater. Interfaces* **2015**, *7*, 10152–10161. [CrossRef] [PubMed]
17. Moratia, N.; Contaret, T.; Gomri, S.; Fiorido, T.; Seguin, J.-L. Noise spectroscopy data analysis-based gas identification with a single MOX sensor. *Sens. Actuators B* **2021**, *334*, 129654. [CrossRef]
18. Gomri, S.; Seguin, J.-L.; Guerin, J.; Aguir, K. Adsorption–desorption noise in gas sensors: Modelling using Langmuir and Wolkenstein models for adsorption. *Sens. Actuators B* **2006**, *114*, 451–459. [CrossRef]
19. Amin, K.R.; Bid, A. Effect of ambient on the resistance fluctuations of graphene. *Appl. Phys. Lett.* **2015**, *106*, 183105. [CrossRef]
20. Rumyantsev, S.; Liu, G.; Shur, M.S.; Potyrailo, R.A.; Balandin, A.A. Selective Gas Sensing with a Single Pristine Graphene Transistor. *Nano Lett.* **2012**, *12*, 2294–2298. [CrossRef]
21. Bhattacharyya, P. Fabrication Strategies and Measurement Techniques for Performance Improvement of Graphene/Graphene Derivative Based FET Gas Sensor Devices: A Review. *IEEE Sens. J.* **2021**, *21*, 10231–10240. [CrossRef]
22. Jokić, I. Microfluidic Adsorption-Based Biosensors: Mathematical Models of Time Response and Noise, Considering Mass Transfer and Surface Heterogeneity. In *Biosensors-Current and Novel Strategies for Biosensing*; Villarreal-Gómez, L., Ed.; Intech Open: London, UK, 2021; pp. 1–25. [CrossRef]
23. Buckley, D.J.; Black, N.C.G.; Castanon, E.G.; Melios, C.; Hardman, M.; Kazakova, O. Frontiers of graphene and 2D material-based gas sensors for environmental monitoring. *2D Mater.* **2020**, *7*, 032002. [CrossRef]
24. Lee, Z.Y.; bin Hawari, H.F.; bin Djaswadi, G.W.; Kamarudin, K. A Highly Sensitive Room Temperature CO_2 Gas Sensor Based on SnO_2-rGO Hybrid Composite. *Materials* **2021**, *14*, 522. [CrossRef] [PubMed]
25. Chen, G.; Paronyan, T.M.; Harutyunyan, A.R. Sub-ppt gas detection with pristine graphene, Appl. *Phys. Lett.* **2012**, *101*, 053119. [CrossRef]
26. Wu, J.; Feng, S.; Li, Z.; Tao, K.; Chu, J.; Miao, J.; Norford, L.K. Boosted sensitivity of graphene gas sensor via nanoporous thin film structures. *Sens. Actuators B* **2018**, *255*, 1805–1813. [CrossRef]
27. Nemade, K.R.; Waghuley, S.A. Chemiresistive gas sensing by few-layered graphene. *J. Electron. Mater.* **2013**, *42*, 2857–2866. [CrossRef]
28. Langmuir, I. The adsorption of gases on plane surfaces of glass, mica and platinum. *J. Am. Chem. Soc.* **1918**, *40*, 1361–1403. [CrossRef]
29. Schuck, P.; Zhao, H. The Role of Mass Transport Limitation and Surface Heterogeneity in the Biophysical Characterization of Macromolecular Binding Processes by SPR Biosensing. *Methods Mol. Biol.* **2010**, *627*, 15–54. [CrossRef] [PubMed]
30. Robinson, J.T.; Perkins, F.K.; Snow, E.S.; Wei, Z.; Sheehan, P.E. Reduced Graphene Oxide Molecular Sensors. *Nano Lett.* **2008**, *10*, 3137–3140. [CrossRef]
31. Gautam, M.; Jayatissa, A.H. Adsorption kinetics of ammonia sensing by graphene films decorated with platinum nanoparticles. *J. Appl. Phys.* **2012**, *111*, 094317. [CrossRef]
32. Noei, M. DFT study on the sensitivity of open edge graphene toward CO_2 gas. *Vacuum* **2016**, *131*, 194–200. [CrossRef]
33. Zhang, Q.; Xu, Y.; Zhang, J.; Lu, Y.; Tian, J. Graphene functionalized by doping and defects for gas sensor application. *Sens. Mater.* **2021**, *33*, 1411–1429. [CrossRef]
34. Alzate-Carvajal, N.; Luican-Mayer, A. Functionalized Graphene Surfaces for Selective Gas Sensing. *ACS Omega* **2020**, *5*, 21320−21329. [CrossRef] [PubMed]
35. Promthong, N.; Tabtimsai, C.; Rakrai, W.; Wanno, B. Transition metal-doped graphene nanoflakes for CO and CO_2 storage and sensing applications: A DFT study. *Struct. Chem.* **2020**, *31*, 2237–2247. [CrossRef]
36. Wang, N.; Yang, S.; Lan, Z.; Xu, H.; Wang, Z.; Hu, Y.; Gu, H. A DFT study of the selective adsorption of XO_2 (X = C, S or N) on Ta-doped graphene. *Comput. Theor. Chem.* **2020**, *1190*, 113003. [CrossRef]
37. Zheng, Z.; Wang, H. Different elements doped graphene sensor for CO_2 greenhouse gases detection: The DFT study. *Chem. Phys. Lett.* **2019**, *721*, 33–37. [CrossRef]
38. Khudair, S.; Jappor, H. Adsorption of Gas Molecules on Graphene Doped with Mono and Dual Boron as Highly Sensitive Sensors and Catalysts. *J. Nanostruct.* **2020**, *10*, 217–229. [CrossRef]
39. Rad, A.S.; Foukolaei, V.P. Density functional study of Al-doped graphene nanostructure towards adsorption of CO, CO_2 and H_2O. *Synth. Met.* **2015**, *210*, 171–178. [CrossRef]
40. Cortés-Arriagada, D.; Villegas-Escobar, N.; Ortega, D.E. Fe-doped graphene nanosheet as an adsorption platform of harmful gas molecules (CO, CO_2, SO_2 and H_2S), and the co-adsorption in O_2 environments. *Appl. Surf. Science* **2018**, *427*, 227–236. [CrossRef]
41. Wood, B.C.; Bhide, S.Y.; Dutta, D.; Kandaga, V.S.; Deep Pathak, A.; Punnathanam, S.N.; Ayappa, K.G.; Narasimhan, S. Methane and carbon dioxide adsorption on edge-functionalized graphene: A comparative DFT study. *J. Chem. Phys.* **2012**, *137*, 054702. [CrossRef]
42. Lee, K.-J.; Kim, S.-J. Theoretical Investigation of CO_2 Adsorption on Graphene. *Bull. Korean Chem. Soc.* **2013**, *34*, 3022–3026. [CrossRef]
43. Vanin, M. First-principles calculations of graphene nanoribbons in gaseous environments: Structural and electronic properties. *Phys. Rev. B* **2010**, *82*, 195411. [CrossRef]

44. Okada, S. Energetics of nanoscale graphene ribbons: Edge geometries and electronic structures. *Phys. Rev. B* **2008**, *77*, 041408. [CrossRef]
45. Koskinen, P.; Malola, S.; Häkkinen, H. Evidence for graphene edges beyond zigzag and armchair. *Phys. Rev. B* **2009**, *80*, 073401. [CrossRef]
46. Dana, S.; Varma, M.M. Gas-Selective Signal Amplification in Fluctuation-Based Graphene FET Sensors. *IEEE Sensors J.* **2016**, *16*, 6533–6536. [CrossRef]
47. Lazar, P.; Otyepková, E.; Banáš, P.; Fargašová, A.; Šafářová, K.; Lapčík, L.; Pechoušek, J.; Zbořil, R.; Otyepka, M. The nature of high surface energy sites in graphene and graphite. *Carbon* **2014**, *73*, 448–453. [CrossRef]